Scientific Visualization, 2026, volume 18, number 1, pages 9 - 19, DOI: 10.26583/sv.18.1.02

Using Sperm Imaging with Laser Interference Microscopy for Comprehensive Assessment of the Functional State of Cells during Cryopreservation and under the Action of Molecular Hydrogen

A.V. Deryugina[1,A], M.N. Ivaschenko[2,A,B], P.S. Ignatiev[3,C], V.B. Metelin[4,D]

[A] Lobachevsky Nizhny Novgorod State University, Nizhny Novgorod, Russia
[B] Nizhny Novgorod State Agrotechnological University named after L.Ya. Florentyev, Nizhny Novgorod, Russia
[C] Production Association «Ural Optical-Mechanical Plant named after E.S. Yalamov», Yekaterinburg. Russia
[D] Moscow Regional Research Clinical Institute named after M.F. Vladimirsky, Moscow, Russia

[1] ORCID: 0000-0001-8812-8559, derugina69@yandex.ru
[2] ORCID: 0000-0001-6642-8518, marina.31@rambler.ru
[3] ORCID: 0000-0001-5075-7034, ignasha2000@yandex.ru
[4] ORCID: 0000-0003-0600-5729, verrv01@gmail.com

Abstract

Significant advances have been made in sperm cryopreservation but the search for effective sperm cryopreservation technologies is a pressing issue in modern biology and medicine. The most effective cryopreservation leaves 50-60% of viable cells. The paper discusses the use of molecular hydrogen (H_2) as a new approach to enhancing sperm protection during freezing and thawing. H_2 is a universal antioxidant and limits damage to biomolecules. Visual registration of spermatozoa under the action of H_2 was performed using modern microscopy techniques. Laser interference microscopy was used in the work. Laser interference microscopy records the cell surface architectonics depending on the modulation of the optical density of cellular structures. This visualization option provides information on the metabolic level and expands the possibilities for interpreting experimental results. Sample preparation, dyes, and fixatives are not used in interference visualization. The paper presents an analysis of phase images of spermatozoa during cryopreservation and using H_2 as a cryoprotector. Verification of the method for analyzing phase characteristics of spermatozoa as an indicator of the metabolic state of cells was performed by analyzing clinical and laboratory parameters of spermatozoa. The phase height of spermatozoa during cryopreservation decreased, the intensity of energy processes decreased, and the oxidative potential of cells increased. A direct correlation was shown between the phase height of spermatozoa and the concentration of ATP, and an inverse correlation was found from the concentration of malondialdehyde (MDA). The use of H_2 determined an increase in the phase height of spermatozoa, an increase in energy metabolism, and a decrease in cell oxidation. Changes in the metabolic activity of spermatozoa under the action of H_2 were combined with an improvement in sperm fertility. Thus, phase interference microscopy allows for a qualitative and quantitative assessment of the physiological state of spermatozoa. It is an objective method of vital analysis of complex metabolic activity of cells. It can be used for express diagnostics of their functional state.

Keywords: phase interference microscopy, diagnostic, sperm, molecular hydrogen.

1. Introduction

The technology of sperm cryopreservation, despite the wide variety of cryoprotectors, is not perfect. The cryopreservation process leads to a loss of approximately 50% of sperm viability [1]. The role of sperm cryopreservation is associated with maintaining the initial motility of sperm and preserving metabolism. However, during the process of cell cryopreservation, damage to proteins, lipids and nucleic acids is observed [2, 3, 4]. Oxidative processes increase during cryopreservation. Free radicals damage cellular and subcellular structures, which reduces cell viability [5]. Oxidative processes are triggers of morphological and biochemical cryogenic damage, cause sperm dysfunction and determine the need for the use of antioxidants. Antioxidants limit the effect of the oxidation process. The use of molecular hydrogen (H_2) as a universal antioxidant is widely discussed today, and its therapeutic effect based on antioxidant properties is considered in various fields of medicine [6, 7]. However, the rationale for the effectiveness of using H_2 in cryopreservation has not yet been presented in modern literature. An objective assessment of the effect of H_2 is possible when conducting a comprehensive analysis of the state of spermatozoa. Interference methods of optical microscopy allow studying cellular processes [8]. Visualization of structural and morphological changes in cells with high spatial resolution is an informative way to study the physiological and biomechanical properties of cells [9]. Interference laser microscopy and interference images make it possible to evaluate transparent bioobjects with an analysis of the density of intracellular structures [10].

The aim of the work was to study the morpho-functional state of spermatozoa during cryopreservation under the action of H2 using laser interference microscopy.

2. Analysis of biological objects in interference microscopy

Interference microscopy analyzes the morphology of an object depending on the refractive index of the intracellular structures of cells. The result of interference microscopy is the registration of the optical density of an object by a direct and reflected beam of light. This is a fundamental difference from conventional light microscopy. Conglomerates and dense structures determine an increase in the refractive index and the registration of convex domains. Oblique illumination from different angles is used for registration (Fig. 1). The phase reconstruction is carried out using the phase step method [11]. In this case, the photodetector registers the displacement of the studied object beam relative to the reference beam with a known phase, which represents the interferogram of the object.

The calculation of the spatial distribution of the intensity of the resulting object in the plane is carried out according to the following formula:

$$I(x) = Ir + Is(x) + 2\sqrt{IrIs(x)}\cos(qx + \phi(x)) \quad (1)$$

Where Ir and Is are the intensities in the reference and object arms of the interferometer, q is the spatial frequency of the fringes, φ is the phase associated with the object.

Fig. 1. Automated interference microscope. 1 – automated two-coordinate stage; 2 – support mirror on piezoelectric element; 3.5 – CCD cameras; 4 – microinterferometer; 6 – laser illuminator.

For transparent objects, Is(x) has a weak dependence on x. By adjusting the magnification of the system, it is possible to select a frequency q close to or greater than the maximum frequency of the interference fringes, limited by the numerical aperture of the objective, so that the fundamental diffraction resolution of the resolving power is preserved. The interference term can be separated by high-pass Fourier filtering. It follows that the complex analytical signal associated with the real function u(x) can be obtained as

$$z(x) = \frac{1}{2}u(x) = i\frac{P}{2\pi}\int_{-\infty}^{+\infty}\frac{U(x')}{x-x'}dx' \qquad (2)$$

In equality (2), using the Hilbert transform for u(x), the phase associated with the complex analytical signal z can be represented as follows:

$$\Phi(x) = \tan^{-1}\left\{\mathrm{Im}\left[z(x)\right]/\mathrm{Re}\left[z(x)\right]\right\} \qquad (3)$$

The basic basis of the interference microscope is a modified Mach-Zehnder interferometer. The radiation source in the Mach-Zehnder interferometer is a He-Ne laser [8]. The reference field for creating the interference image is tilted relative to the object beam at an angle of 45° relative to the x and y axes (Fig. 2).

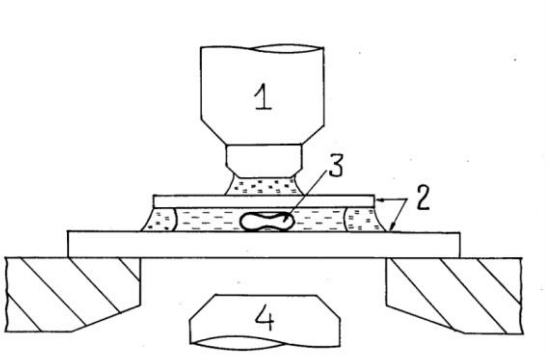

Fig. 2. Schematic representation of the microchamber and (on an enlarged scale) the cell being photometered. 1 – microscope objective, 2 – cover slips, 3 – erythrocyte, 4 – condenser.

The diagram of the laser interference microscope used in this work is shown in Fig. 3. The device includes a light source I, semitransparent mirrors BS1, BS2, BS3, rotating mirrors M1, M2, polarizers WP1, WP2, phase modulator PM, objective O, analyzer A and detector D. Polarizers WP1, WP2 modulate the phases of the reference and object beams. Phase modulator PM forms the phase modulation of the reference beam. The object beam is reflected from the object of study located on the stage S, passes through mirror BS3, mixes with the reference beam and passes through analyzer A, which selects from it a component with one or another polarization, and hits the detector.

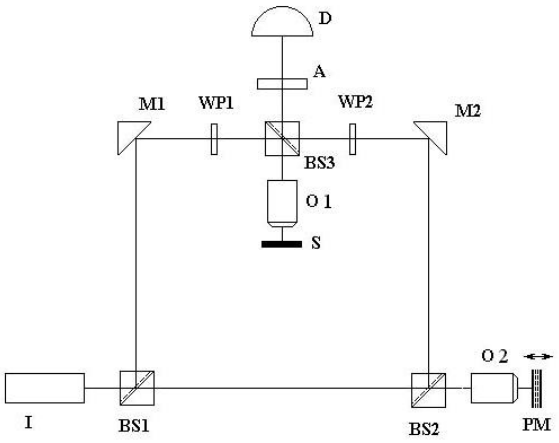

Fig. 3. Schematic diagram of the laser interference microscope interferometer.

The use of an interference laser microscope allows for ultra-high resolution, which reaches 0.1 nm (vertically) and 15 - 100 nm in the plane of the object [12]. Calculation of the interference pattern obtained from the object model allows to represent the expression of the three-dimensional shape of the cells. This method is a new approach to visualization for the analysis of cell morphology and can be useful for studying their unique physiological and biomechanical properties.

3. Object of study

The study involved sperm diluted with the BioXcell medium (France) and then frozen in liquid nitrogen (-196°C) according to GOST 26030-2015. The condition of the spermatozoa was analyzed after defrosting the sperm using standard technology. The study involved sperm diluted with the BioXcell diluent (group I), sperm after deep freezing (group II), and sperm after deep freezing pre-treated with H_2 (group III). The concentration of H_2 in the solution was within 1.2-1.5 mg/l. The hydrogen generator «Sputnik-3» (China) produced H_2.

To assess the qualitative parameters of spermatozoa, we used the SFA-500 and Biola AFS-500 sperm analyzers from NPF BIOLA (Russia). The energy parameters of spermatozoa were assessed by the concentration of ATP using a non-enzymatic method [13]. The antioxidant system was analyzed by the activity of SOD [14] and catalase [15]. The oxidative properties of cells were determined by the concentration of MDA in spermatozoa using a reaction with thiobarbituric acid [16].

Interference laser microscopy was performed on a MIM-340 microscope using a laser with a wavelength of 650 nm. The vertical resolution was 0.1 nm. Interferograms were processed in the MIM Visualizer 1.0 program (MIM Software Inc., USA) [17].

Differences between groups were compared using the Student's t-test with Bonferroni correction, taking into account the significance threshold of $p \leq 0.05$. Correlation analysis was performed using the Spearman correlation coefficient.

4. Results of spermatozoa examination using interference microscopy

The calculated parameters of sperm interforegrams without treatment (group I) were: phase height 24.03±0.02 nm, capitulum and tail length of spermatozoa 9.53±0.62 μm and 46.82±5.25 μm, respectively (Table 1). Cryopreservation determined a decrease in the capitulum and tail length in 7.01% and 9.53% of spermatozoa, respectively ($p \leq 0.05$). The use of H_2 in the cryopreservation process led to the preservation of the optical and geometric parameters of spermatozoa at the level of native cells (group I).

Table 1. The effect of cryopreservation and molecular hydrogen on the optical-geometric parameters of spermatozoa

Sperm Parameters	Native spermatozoa (group I)	Spermatozoa after cryopreservation (group II)	Spermatozoa after exposure to molecular hydrogen and cryopreservation (group III)
Capitulum length, μm	9,53±0,62	8,32±0,55*	9,04 ±0,49 $^{\Delta}$
Tail length, μm	46,82±2,05	42,36±2,35 *	45,74± 1,59 $^{\Delta}$
Phase height, nm	24,03±0,02	21,32±0,05*	23,04 ±0,04*, $^{\Delta}$

Note: * – differences in relation to group I, $p \leq 0.05$; Δ – differences between groups after cryopreservation (group II and group III).

Figure 4 shows typical phase portraits of spermatozoa exposed to H_2 during cryopreservation and without H_2 during cryopreservation. Analysis of phase interference images of spermatozoa showed that after H_2 exposure the capitulum was oval-shaped, the middle part of the

cell was thin and the tail was straight. The acrosomal region after exposure to molecular hydrogen was well defined and occupied from 40 to 70% of the cell. This distribution of the acrosome corresponds to the physiological norm, since the acrosome was shown to cover about 2/3 of the anterior surface of the head. Determination of the acrosome status in cryopreserved sperm is of fundamental importance, since cryopreservation directly damages the sperm membranes which can lead to the loss of the contents of the acrosomal matrix. After cryopreservation without H_2, uneven distribution of cytoplasm in the capitulum with abnormal acrosome was noted. This indicates a change in the permeability of the plasma membrane and loss of the ability to attach to the oocyte membrane. The loss of acrosomal matrix content reduces the longevity of cryopreserved spermatozoa [18].

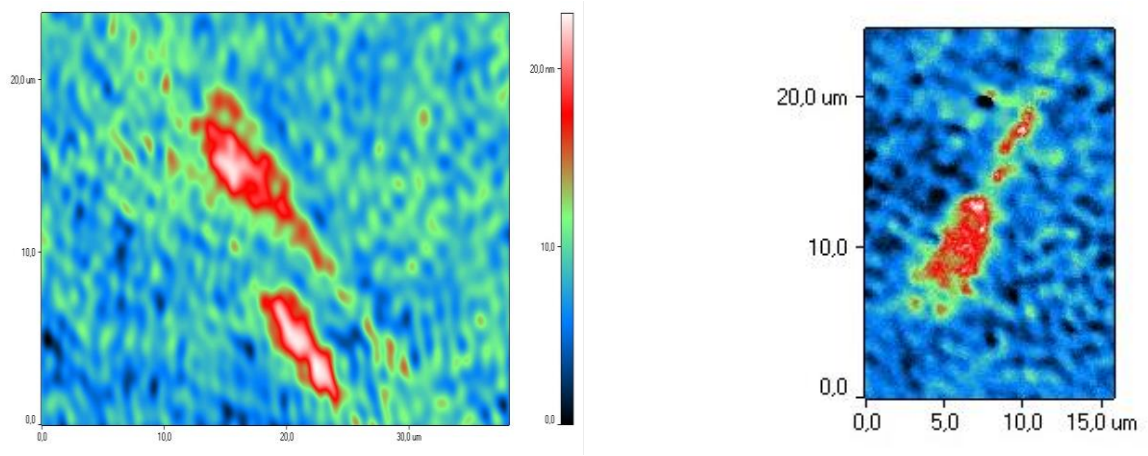

a) b)

Fig. 4. Typical phase images of spermatozoa after cryopreservation using H_2 (a) and after cryopreservation without H_2 (b).

Evaluation of phase heights of sperm interphoregrams and changes in the refractive index allowed us to estimate the distribution of the substance density in the cells. The phase height in the plane represents the spatial modulation of the wave from a coherent source. Different refractive indices of parts of the cell are transformed into a two-dimensional distribution of the optical component [19].

The analysis of the sperm profile showed the presence of a phase peak in the region of the initial head segment in native spermatozoa and under the action of H_2 during cryopreservation (Fig. 5a, 5c). This indicates the maximum density in the acrosomal region. The phase height in the acrosome region of native spermatozoa and during cryopreservation with H_2 significantly exceeded the phase height in spermatozoa during cryopreservation without H_2 (Fig. 5). This region corresponds to the nucleus with the nucleolus. However, the decrease in the phase height of spermatozoa during cryopreservation without H_2 indicates a decrease in the density in this region of the cell. The low density is probably due to protein loss. Proteins are involved in fertilization processes: motility, acrosome reaction, fusion with the egg [20]. Changes in the protein composition of the sperm membrane are one of the main reasons for the decrease in sperm fertility after cryopreservation.

This position is confirmed by previously identified facts obtained using interference microscopy, indicating that the change in phase height is proportional to the product of the membrane thickness and the difference in the local refractive index of the cell and the solution [21].

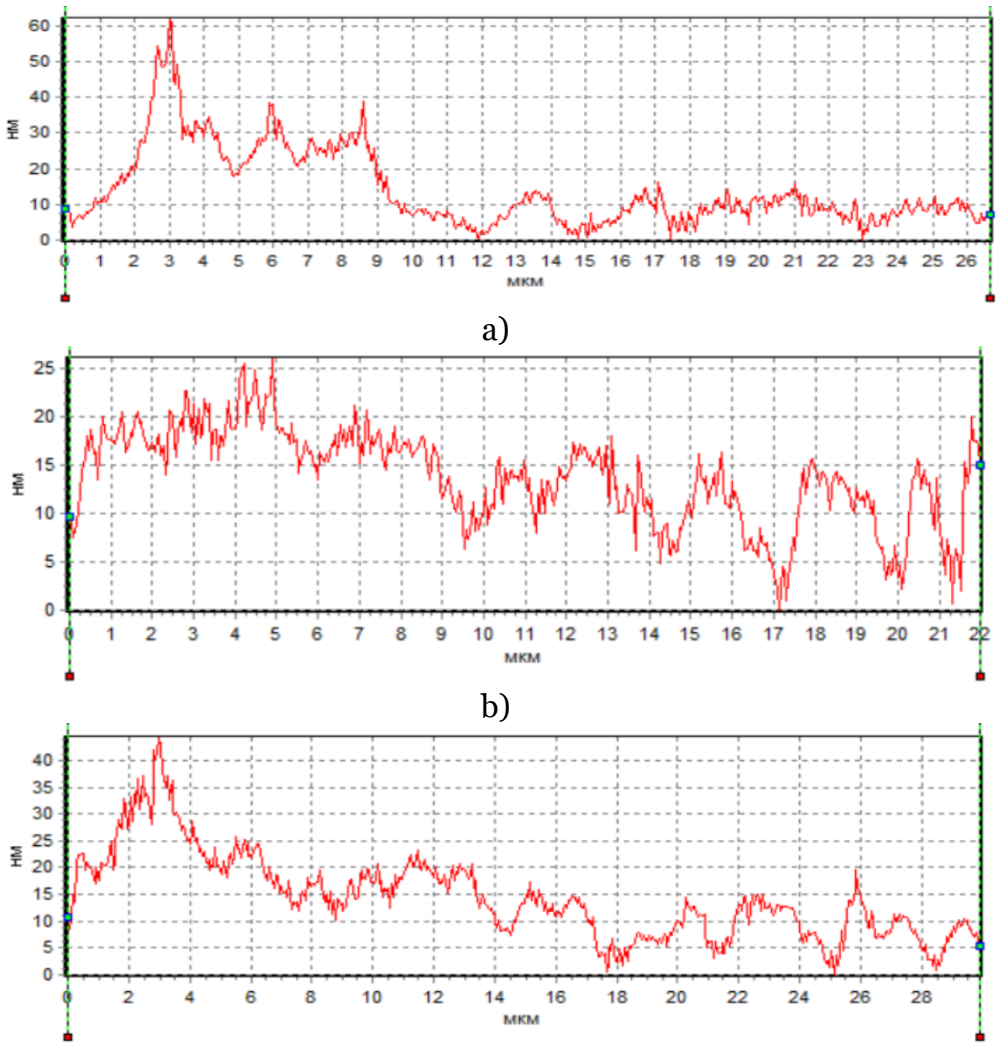

Fig. 5. Profiles of changes in the phase height of spermatozoa: intact (a), after cryopreservation without H_2 (b) and after cryopreservation using H_2 (c).

In our experiments, a decrease in the phase height of spermatozoa was observed during cryopreservation (Fig. 5b). Apparently, this is due to damage to spermatozoa during cryopreservation and their subsequent thawing. In particular, it was noted that phase heights decrease proportionally to the degree of damage and an increase in the amount of water inside the cell, which leads to a decrease in the refractive index due to the loss of concentration of the substance inside [22]. Destruction of the plasma membrane during cryopreservation can cause further damage to cells and, consequently, lead to irreversible damage to their integrity. In many ways, this development of events can be due to oxidative processes and changes in cell metabolism, since interforegrams reflect the dynamics of various intracellular processes [23]. To substantiate the stated position, we conducted biochemical studies of intracellular metabolism in parallel with the interference registration of cells.

5. Results of the study of functional and biochemical parameters of spermatozoa

A study of the oxidative metabolism level revealed that cryopreservation was accompanied by a significant increase in the lipid peroxidation process, which was characterized by an increase in the concentration of malondialdehyde (MDA) by 39% relative to native spermatozoa (group I) (Table 2). The use of H_2 in the cryopreservation process made it possible to maintain the intensity of oxidative processes at the level of native spermatozoa.

Table 2. Oxidative and metabolic activity of spermatozoa during cryopreservation and exposure to molecular hydrogen

Indicators	Native spermatozoa (group I)	Spermatozoa after cryopreservation (group II)	Spermatozoa after exposure to molecular hydrogen and cryopreservation (group III)
MDA, nmol/ml	0,61±0,12	0,85±0,14 *	0,56±0,08 $^{\Delta}$
SOD, units/mg protein	0,61±0,08	0,78±0,08 *	0,87±0,08 *,$^{\Delta}$
Catalase, mcat/mg	9,03±0,76	8,48±0,82	15,78±0,71 *,$^{\Delta}$
ATP, μmol/l	0,79±0,09	0,28 ±0,05 *	0,47±0,04 *, $^{\Delta}$

Note: * – differences in relation to group I, p≤0.05; Δ – differences between groups after cryopreservation (group II and group III).

The inhibiting factor of oxidative processes is the increase in the activity of antioxidant enzymes. The activity of SOD and catalase in spermatozoa increased after the addition of H_2 to the cryopreservation medium (group III) (Table 3). The activity of SOD and catalase increased by 42% and 74%, respectively (p≤0.05) relative to native spermatozoa (group I).

The ATP concentration in spermatozoa after cryopreservation was lower than in native spermatozoa (group I) by 65%. The ATP content in spermatozoa increased by 67% during cryopreservation with H2 (group III) relative to group II.

A correlation dependence was revealed between the metabolic indices and the phase characteristics of spermatozoa during cryopreservation and the use of H_2 against the background of cryopreservation (Table 3). Analysis of the correlation dependences between the phase height and the oxidative metabolism index revealed a close negative correlation in all groups (R=-0.88 – Group I, R=-0.85 – Group II, R=-0.93 – Group III) and a strong correlation between the phase height and the energy metabolism index (R=0.88 – Group I, R=0.85 – Group II, R=0.93 – Group III).

Table 3. Correlation analysis of phase height and metabolic indices in different groups

	Phase Height/MDA	Phase Height/ATP
Native spermatozoa (group I)	-0,88	0,84
Spermatozoa after cryopreservation (group II)	-0,85	0,86
Spermatozoa after exposure to molecular hydrogen and cryopreservation (group III)	-0,93	0,91

Correlation relationships prove that the analysis of the phase height of spermatozoa obtained by interference microscopy allows us to evaluate the total metabolic activity of spermatozoa and has the highest sensitivity compared to biochemical methods.

When analyzing the results obtained, it should be taken into account that during cryopreservation, lipids and proteins in a liquid state harden, turning into a gel, forming a rigid and fragile structure that is more sensitive to damage [24]. Our study shows that during cryopreservation, there is a loss of integrity of both acrosomal and plasma membranes. During freezing, spermatozoa undergo significant metabolic changes and mitochondrial function is greatly impaired [25]. The bioenergetic function of mitochondria plays an important role in spermatozoa, especially for capitation, hyperactivation and acrosome reaction [26]. The obtained results demonstrate that the use of H_2 is effective in protecting sperm metabolism during cryopreservation. The use of H_2 can ensure the preservation of sperm functional parameters.

The study showed that the use of H_2 during cryopreservation maintained the number of motile spermatozoa, the number of fast spermatozoa, and the average speed of spermatozoa

at the level of native cells (Table 4). Whereas after cryopreservation of spermatozoa, these indicators were reduced.

Table 4. Effect of molecular hydrogen on sperm fertility parameters

Sperm Fertility Criteria	Native spermatozoa (group I)	Spermatozoa after cryopreservation (group II)	Spermatozoa after exposure to molecular hydrogen and cryopreservation (group III)
Mobility, %	82,51±3,95	71,15±3,34 *	79,62±3,60 $^{\Delta}$
Number of mobile, million/dose	35,76±2,17	27,35±2,16*	33,71±2,03 $^{\Delta}$
Number of fast, million/dose	65,54±7,14	51,77±6,13*	58,98±6,55$^{\Delta}$
Average speed, μm/sec	85,62±3,54	74,53±2,48*	81,56±3,52 $^{\Delta}$

Note: * – differences in relation to group I, $p \leq 0.05$; Δ – differences between groups after cryopreservation (group II and group III).

Considering that the speed of sperm movement is one of the most informative indicators of sperm quality [27], the detected increase in the number of motile, fast spermatozoa and the average speed of spermatozoa under the influence of H2 compared to these indicators during cryopreservation proves the effectiveness of using H2 as a cryoprotector.

Conclusions

1. The study demonstrated the effectiveness of using H_2 as a new strategy for protecting spermatozoa during cryopreservation.
2. Analysis of spermatozoa interforegrams provides a comprehensive assessment of the state of spermatozoa metabolic processes during cryopreservation.
3. Phase images allow for clear identification of spermatozoa with a reduced functional state which can be used for express analysis of spermatozoa quality.

Acknowledgments

This work was supported by the Russian Science Foundation (project No. 23-26-00205).

References

1. Watson P.F. The causes of reduced fertility with cryopreserved semen // Anim Reprod Sci. 2000. № 60–61. P. 481–92. doi: 10.1016/s0378-4320(00)00099-3.
2. Sion B., Janny L., Boucher D., Grizard G. Annexin V binding to plasma membrane predicts the quality of human cryopreserved spermatozoa // Int J Androl. 2004. №27 (2). P. 108–1014. doi: 10.1046/j.1365-2605.2003.00457.x.
3. Kogan T., Dahan D.G., Laor R., Argov-Argaman N., Komsky-Elbaz A., Kalo D., Roth Z. Association between Fatty Acid Composition, Cryotolerance and Fertility Competence of Progressively Motile Bovine Spermatozoa // Animals (Basel). 2021. №11 (10). P. 2948. doi: 10.3390/ani11102948.
4. Thomson L.K., Fleming S.D., Aitken R.J., De Iuliis G.N., Zieschang J.A., Clark A.M. Cryopreservation-induced human sperm DNA damage is predominantly mediated by oxidative stress rather than apoptosis // Hum Reprod. 2009. № 24(9). P. 2061–70. doi: 10.1093/humrep/dep214
5. Partyka A., Lukaszewicz E., Niżański W., Twardoń J. Detection of lipid peroxidation in frozen-thawed avian spermatozoa using C(11)-BODIPY(581/591) // Theriogenology. 2011. №75 (9). P. 1623–9. doi: 10.1016/j.theriogenology.2011.01.002.

6. Zhai X., Chen X., Shi J., Shi D., Ye Z., Liu W. Lactulose ameliorates cerebral ischemia-reperfusion injury in rats by inducing hydrogen by activating Nrf2 expression // Free Radic. Biol. Med. 2013. № 65. P. 731–741. doi: 10.1016/j.freeradbiomed.2013.08.004

7. Miller M. W., Sadeh N. Traumatic stress, oxidative stress and post-traumatic stress disorder: neurodegeneration and the accelerated-aging hypothesis // Mol. Psychiatry 2014. № 19. P. 1156–1162. doi: 10.1038/mp.2014.111

8. Lue N., Popescu G., Ikeda T., Dasari R., Badizadegan K., Feld M. Live cell refractometry using microfluidic devices // Opt. Lett. 2006. № 31(18). P. 2759-2761. doi: 10.1364/ol.31.002759

9. Park Y., Popescu G., Badizadegan K., Dasari R., Feld M. Diffraction phase and fluorescence microscopy // Opt. Expr. 2006. № 14(18). P. 8263-8268. doi: 10.1364/oe.14.008263

10. Levin G.G., Bulygin F.V., Vishnyakov G.N. Coherent oscillations of the state of protein molecules in living cells // Tsitology. 2005. V.47. №4. P.348-356.

11. Deryugina A.V., Ivaschenko M.N., Ignatiev P.S., Metelin V.B., Talamanova M.N. Possibilities of intravital visualization of blood cells under stress to assess the state of the body // Scientific visualization.2023. V. 15. № 1. P. 90-99. doi: 10.26583/sv.15.1.08

12. Tychinsky V.P., Kretushev A.V., Klemyashov I.V., Vyshenskaya T.V., Shtil A.A., Zatsepina O.V. Coherent phase microscopy – a new approach to studying the physiological state of the nucleolus // DAN. 2005. № 405(4). P. 432-436.

13. Deryugina A.V., Danilova D.A., Pichugin V.V., Brichkin Yu.D. The effect of molecular hydrogen on functional states of erythrocytes in rats with simulated chronic heart failure // Life. 2023. №3(13). P. 418. doi: 10.3390/life13020418

14. Sirota T.V. Standardization and regulation of the rate of superoxide-generating reaction of adrenaline autoxidation used to determine the pro/antioxidant properties of various materials // Biomedical Chemistry. 2016. № 6. P. 650–655. doi: 10.18097/PBMC20166206650

15. Deryugina A.V., Abaeva O.P., Romanov S.V., Vedunova M.V., Ryabova E.N., Vasenin S.A., Titova N.A. Electrokinetic, oxidative and aggregation properties of red blood cells in the postoperative period following kidney transplantation // Russian journal of transplantology and artificial organs. 2020. № 2. P. 72-79. doi: 10.15825/1995-1191-2020-2-72-79

16. Deryugina A.V., Efimova T.S., Boyarinov G.A., Nikolskiy V.O., Kuznetsov A.B., Simutis I.S. Correction of metabolic indicators of erythrocytes and myocardium structure with ozonized red blood-cell mass // Cell and Tissue Biology. 2018. V. 12. № 3. P. 207-212. doi: 10.1134/S1990519X18030033

17. Deryugina A.V., Belov A.A., Ivashchenko M.N., Ignatiev P.S., Metelin V.B. Assessing the functional state of red blood cells by using the laser interference microscopy // Cell and Tissue Biology. 2021. V. 15. № 4. P. 388-392. doi: 10.1134/S1990519X21040027

18. Bailey J.L., Bilodeau J.F., Cormier N. Semen cryopreservation in domestic animals: a damaging and capacitating phenomenon // J. Androl. 2000. № 21. P. 1-7.

19. 19. Tychinsky V. P. Dynamic phase microscopy: is a “dialogue” with a cell possible? // Uspekhi Fizicheskikh Nauk. 2007. №5 (177). P. 535–552 doi: 10.3367/UFNr.0177.200705c.0535

20. Kondoh G., Tojo H., Nakatani Y., Komazawa N., Murata C., Yamagata K., Maeda Y., Kinoshita T., Okabe M., Taguchi R. Takeda J. Angiotensin-Converting Enzyme Is a GPI-Anchored Protein Releasing Factor Crucial for Fertilization // Nature Medicine. 2005. № 11. P. 160-166. https://doi.org/10.1038/nm1179.

21. Yusipovich A.I., Berestovskaya Yu.Yu., Shutova V.V., Levin G.G., Gerasimenko L.M., Maksimov G.V., Rubin A.B. New possibilities of studying microbiological objects by laser interference microscopy // Biophysics. 2011. V. 56. № 6. P. 1091–1098.

22. Zagubizhenko M.V., Yusipovich A.I., Pirutin S.K., Minaev V.L., Kudryashov Yu.B. Using the method of laser interference microscopy to study the state of mouse peritoneal macrophages irradiated with ultraviolet light // Radiation biology. Radioecology. 2011. № 6(51). P. 715–720

23. Brazhe A.R., Brazhe N.A., Sosnovtseva O.V., Pavlov A.N., Mozekilde E., Maksimov G.V. Study of cellular dynamics using interference microscopy with wavelet analysis // Computer research and modeling. 2009. V. 1. № 1. P. 77–83

24. Gao D., Critser J.K. Mechanisms of cryoinjury in living cells // ILAR J. 2000. №41(4). P. 187–96. doi: 10.1093/ilar.41.4.187.

25. Schober D., Aurich C., Nohl H., Gille L. Influence of cryopreservation on mitochondrial functions in equine spermatozoa // Theriogenology. 2007. № 68. P. 745–54. doi: 10.1093/ilar.41.4.187.

26. O'Flaherty C., de Lamirande E., Gagnon C.. Positive role of reactive oxygen species in mammalian sperm capacitation: triggering and modulation of phosphorylation events // Free Radic Biol Med. 2006. № 41(4). P. 528–40. doi: 10.1016/j.freeradbiomed.2006.04.027

27. Lyashenko A.A. Biological parameters of bull sperm depending on the storage period in liquid nitrogen // Zootechnical science of Belarus. 2015. V. 50. №1. C. 126-134.